

ENERGY-CONVERSION EFFICIENCY WITH COUPLED INDUCTOR FOR AC APPLICATIONS

Madhukar Reddy Nimmala¹, Dr. Subhashish Boss²

¹Research Scholar, Dept. of Electrical and Electronics Engineering, Sri Satya Sai University of Technology & Medical Sciences, Sehore, Bhopal-Indore Road, Madhya Pradesh, India.

²Research Guide, Dept. of Electrical and Electronics Engineering, Sri Satya Sai University of Technology & Medical Sciences, Sehore, Bhopal Indore Road, Madhya Pradesh, India.

Received: 14.01.2020

Revised: 17.02.2020

Accepted: 09.03.2020

ABSTRACT: Dual-stage micro-inverters are commonly utilized in grid-associated photovoltaic (PV) frameworks. The high advance DC/DC converter is basic for the grid-associated micro-inverter in light of the fact that the information voltage from a single solar panel is exceptionally small. A DC/DC coupled inductor with Zeta converter which works at moderate obligation proportions is proposed. High voltage gain is accomplished by utilizing a high go's proportion to the coupled inductor. The leak inductor energy of the coupled inductor is proficiently reused to the load by extra capacitors and diodes and consequently effective energy-conversion is conceivable. The weight on the dynamic switch is likewise limited. Coupled inductor with Zeta converter is simulated and voltage conversion proportion of 8 is acquired. AC produce voltage is assimilated by associating it to an inverter. The voltage addition of 8 and a productivity of 65% are accomplished for the proposed framework.

KEYWORDS: Zeta converter, Energy, Coupled inductor.

© 2020 by Advance Scientific Research. This is an open-access article under the CC BY license (<http://creativecommons.org/licenses/by/4.0/>) DOI: <http://dx.doi.org/10.31838/jcr.07.04.307>

I. INTRODUCTION

The reduction on the worlds non-renewable energy source energy and its failure to fulfill the energy need sooner rather than later needs to prompt the utilization of sustainable power source. As the world's photovoltaic market is developing quickly, the job of grid-associated PV frameworks in appropriated energy frameworks will get significant, and the PV inverter will likewise assume a key job in this expanding market [1]. The AC module, which has been proposed to improve these issues, is known as the micro-inverter. Solar micro-inverter is an inverter coordinated into each solar panel module. The dual-stage micro-inverter joins a high advance up DC/DC converter and DC/AC inverter. By utilizing this dual-stage micro-inverter we can accomplish productivity as high as the traditional PV string-type inverter [2]. The DC/DC converters utilized in the dual-stage micro-inverter of the grid-associated PV frameworks require high advance up voltage conversion.

II. ZETA CONVERTER

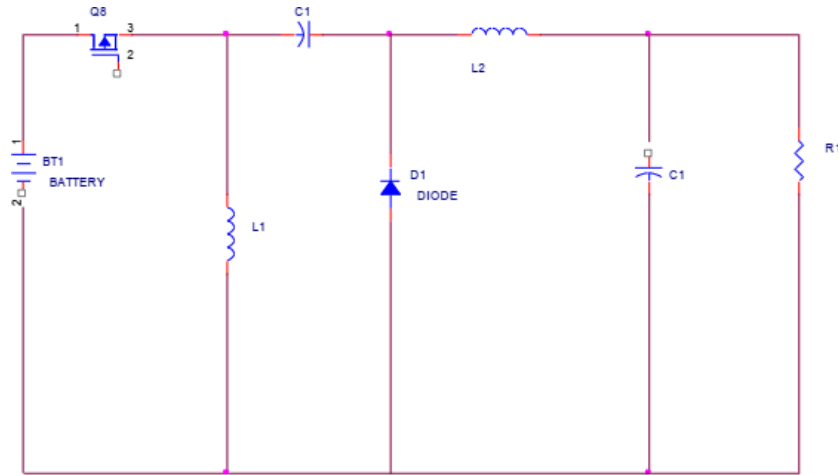


Figure 1: Circuit Diagram of Zeta Converter

A zeta converter is a fourth solicitation nondirect structure being that as to imperativeness enters, it can see as a buck-help buck converter and with regards to the yield, it tends to be seen as an assist buck with supporting converter. Right when the switch is ON (closed), the diode D is OFF. In the midst of this historical, the current through the inductor L1, L2 are strained with the voltage source.

III.PULSE WIDTH MODULATION CONVENTIONAL ZETA CONVERTER

The PWM Zeta converter is a stage up/down converter of non-reversing extremity type and it tends to be intended to accomplish low-swell yield current with isolated inductors [3].

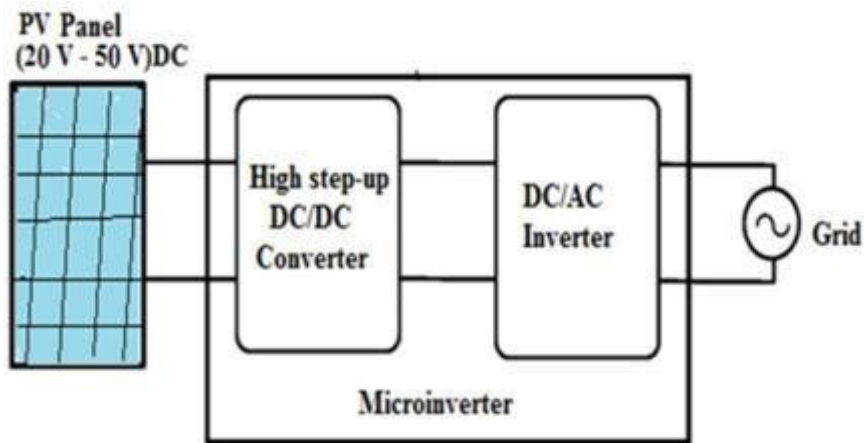


Figure 2: Dual Stage Micro Inverter

Zeta converter is utilized in control factor remedy and voltage guideline plans. The customary Zeta converter is arranged of two inductors, an arrangement capacitor and a diode [4]. The most well-known working methods of these PWM converters are the CICM or CCM and irregular inductor current mode (DICM or DCM).

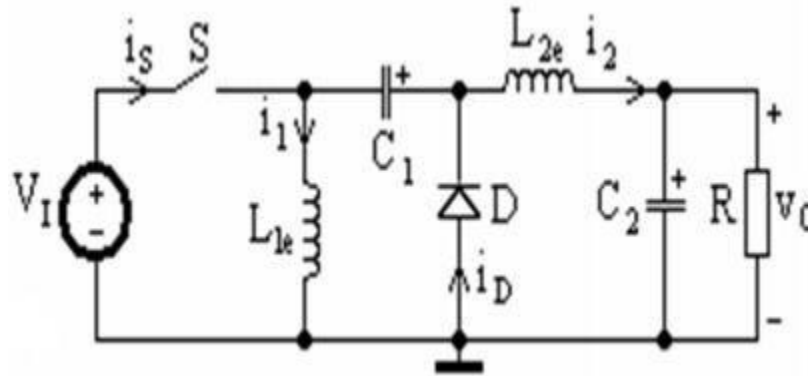


Figure 3: PWM Zeta Converter Circuit Diagram

Expecting 100% effectiveness, the obligation cycle, D_1 , for a Zeta converter working in CCM is given by

$$D_1 = V_0 / (V_i + V_0)$$

Where, V_i and V_o are the input and output voltages of PWM Zeta converter.

Coupled inductor

The coupled inductor comprises of two separate inductors twisted on a similar center; they ordinarily arrive in a bundle with a similar length and width as that of a solitary inductor of similar inductance esteem, just marginally taller. The cost of a coupled inductor is likewise regularly substantially less than the cost of two single inductors. “The windings of the coupled inductor can be associated with the arrangement, in parallel, or as a transformer.

The vast majority of the coupled inductors have a similar number of turns i.e., a 1:1 turns proportion yet some more up to date ones have a higher turn's proportion.

The coupling coefficient, K , of coupled inductors is regularly around 0.95, much lower than a custom transformer's coefficient of more prominent than 0.99.”

The stray inductance of the coupled inductors can be used to control the decay rate of the diode current and reduce the diode recovery problem.

An inductor coupled to a lower voltage switch is used to increase the voltage gain (regardless of whether the switch is on or off). In addition, a latent regenerative damper is used to absorb the energy of the parasitic inductance so that the duty cycle of the switch can be used in a wide range and the associated voltage gain is greater than that of the other converters. coupled inductors.

By replacing information inductors of the DC / DC converters with a cell surrounded by a coupled inductor and a diode, a group of high voltage ratio transducers is generated. The stored energy in the leakage inductance passes through the diode to the pile. As a result, the anxiety when switching is considerably reduced.

Coupled inductor with zeta converter

The circuit arrangement of the proposed DC to DC converter is appeared in Figure 4. This topology is essentially gotten from a traditional Zeta converter by supplanting the information inductor by a coupled inductor.

The turns proportion of the coupled inductor builds the voltage gain and the auxiliary twisting of the coupled inductor is in arrangement with an exchanged capacitor for further expanding the voltage. In Figure 4 S_1 is the coasting dynamic switch.

The essential twisting N_1 of a coupled inductor is like the information inductor of the regular lift converter, then again, actually capacitor C_1 and diode D_1 reuses the leakage-inductor energy from N_1 .

The auxiliary winding N_2 is associated with another pair of capacitor C_2 and diode D_2 which reuses the leakage inductor energy from N_2 . Presently N_2 , C_2 and D_2 every one of the three are in arrangement with N_1 . The diode D_3 interfaces with the yield capacitor C_3 and burden R .

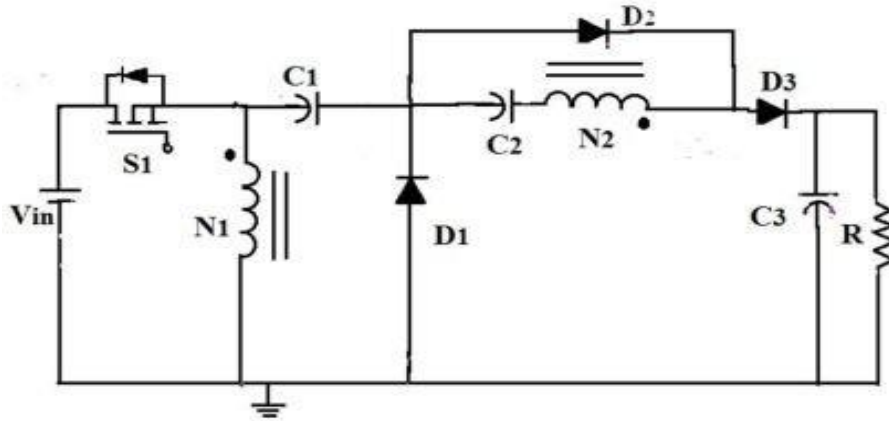


Figure 4: Proposed System Circuit Diagram

Continuous-Conduction Mode Operation Mode 1 [t0, t1]

In the change interim [t0, t1], switch S1 and diode D2 conducts. The source voltage V_{in} is applied on polarizing inductor L_m and essential leakage inductor L_{k1} ; in the mean-time, L_m additionally discharges its energy to the optional winding, and furthermore accuses capacitor C2 along of the reduction in energy. Accordingly the charging current i_{D2} and i_{C2} likewise diminishes.

The auxiliary leakage inductor current i_{Lk2} is decays as indicated by i_{Lm}/n . This mode closes when the expanding i_{Lk1} rises to the diminishing i_{Lm} at $t = t_1$.

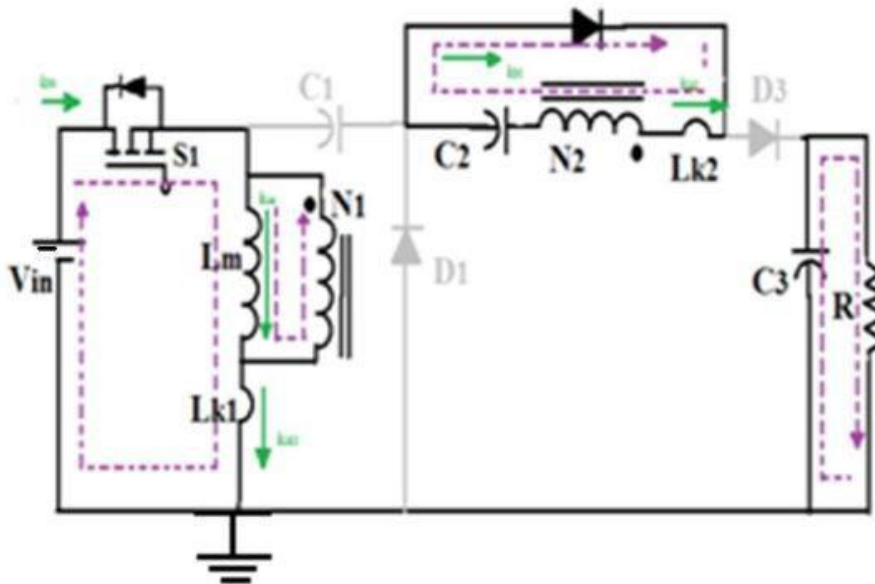


Figure 5: Mode 1 Current Flow Path

Mode II [t1, t2]

In the interim [t1, t2], switch S1 stays ON and diode D3 conducts. The source energy V_{in} is arrangement associated with C1, C2, optional winding N2, and L_{k2} to charge yield capacitor C3 and burden R. In the mean-time, polarizing inductor L_m is additionally gets energy from V_{in} .

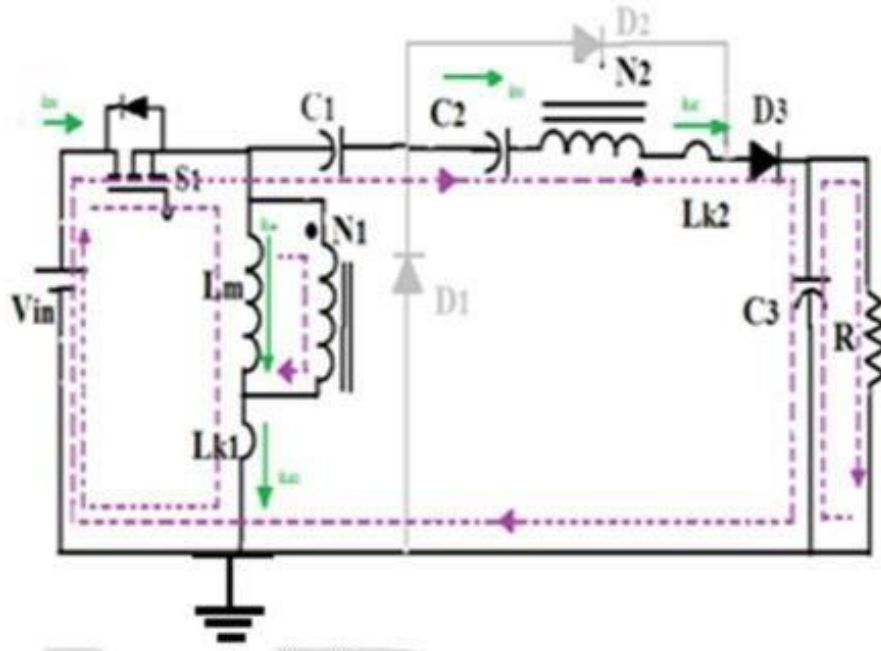


Figure 6: Mode II Current Flow Path

The i_{Lm} , i_{Lk1} , and i_{D3} are expanding in light of the fact that the V_{in} is crossing L_{k1} , L_m and essential winding N_1 .

L_m and L_{k1} are putting away energy from V_{in} ; in the mean-time, V_{in} is additionally in arrangement with N_2 of coupled inductor and capacitors C_1 and C_2 are releasing their energy to capacitor C_3 and burden R , which prompts increment in i_{Lm} , i_{Lk1} , i_{DS} , and i_{D3} . This mode closes when switch S_1 is killed at $t = t_2$.

Mode III [t_2, t_3]

In the interim [t_2, t_3], switch S_1 is killed and just diodes D_1 and D_3 conducts. The present stream way is appeared in Figure.7. The auxiliary leakage inductor L_{k2} continues charging C_3 when switch S_1 is off. The energy put away in leakage inductor L_{k1} moves through diode D_1 to charge capacitor C_1 immediately when S_1 kills. The voltage crosswise over S_1 is the summation of V_{in} , V_{Lm} , and V_{Lk1} . Flows i_{Lk1} and i_{Lk2} are quickly declining, however i_{Lm} is expanding in light of the fact that L_m is getting energy from L_{k2} . When current i_{Lk2} drops to zero, this mode closes at $t = t_3$.

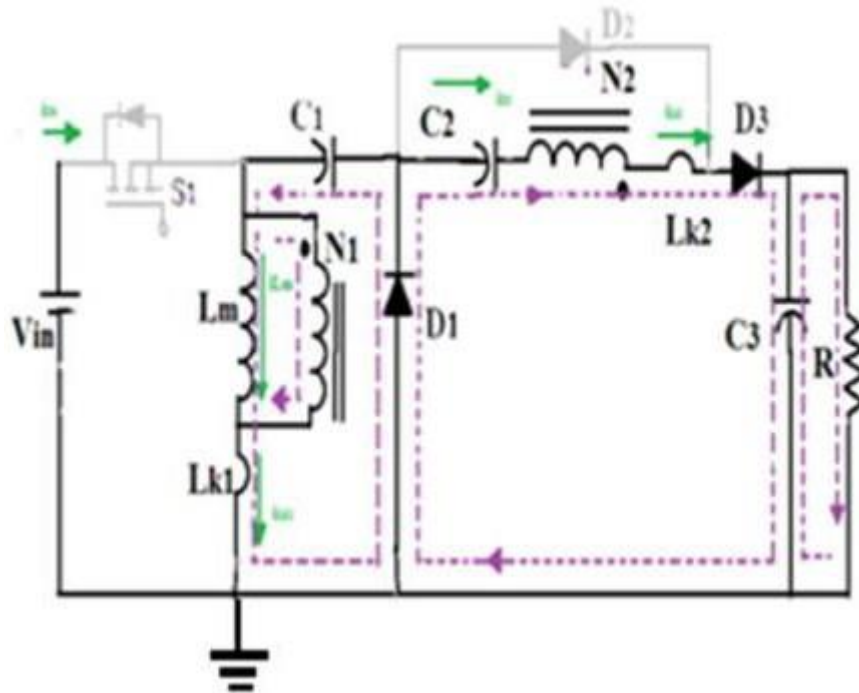


Figure 7: Mode III Current Flow Path

Mode IV [t3, t4]

During the change interim [t3, t4], the energy put away in polarizing inductor L_m discharges all the while to C_1 and C_2 . The present stream way is appeared in Figure 8. Just diodes D_1 and D_2 are directing. Flows i_{Lk1} and i_{D1} are determinedly diminished on the grounds that leakage energy still moves through diode D_1 and keeps charging capacitor C_1 . The L_m is conveying its energy through the coupled inductor and D_2 to charge capacitor C_2 . The energy put away in capacitors C_3 is continually released to the heap R . Flows i_{Lk1} and i_{Lm} are diminishing, yet i_{D2} is expanding. This mode closes when current i_{Lk1} is zero at $t = t_4$.

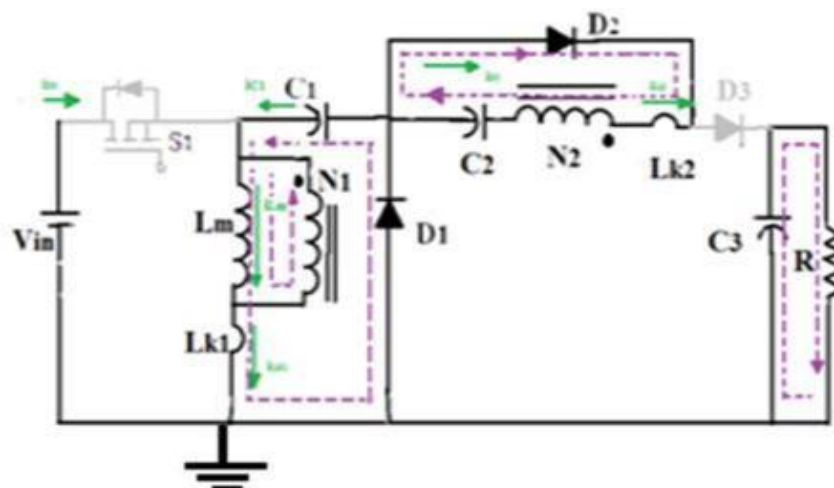


Figure 8: Mode IV Current Flow Path Steady-State Analysis of Proposed Converters

Continuous-conduction mode operation

To rearrange the enduring state investigation, just modes II and IV are considered for CCM activity, and the leakage inductances at essential and optional sides are overlooked.

$$v_{Lm} = V_{in}$$

$$v_{N2} = nV_{in}$$

$$\begin{aligned}
 v_{Lm} &= -V_{C1} \\
 -v_{N2} &= V_{C2} \\
 \int_0^{DT_s} (V_{in})dt + \int_{DT_s}^{T_s} (-V_{C1})dt &= 0 \\
 \int_0^{DT_s} (nV_{in})dt + \int_{DT_s}^{T_s} (-V_{C2})dt &= 0 \\
 V_{C1} &= \frac{D}{1-D} V_{in} \quad V_{C2} = \frac{nD}{1-D} V_{in} \\
 V_O &= V_{in} + \frac{D}{1-D} V_{in} + nV_{in} + \frac{nD}{1-D} V_{in} = \frac{1+n}{1-D} V_{in} \\
 M_{CCM} &= \frac{V_O}{V_{in}} = \frac{I_{in}}{I_O} = \frac{1+n}{1-D}
 \end{aligned}$$

MCCM as part of the translation report (D) for various gear ratios (n) is shown in a diagram, and the straightness of the curve represents the solution between the gear ratio and the duty cycle (D) represents the voltage gain MCCM = 8.

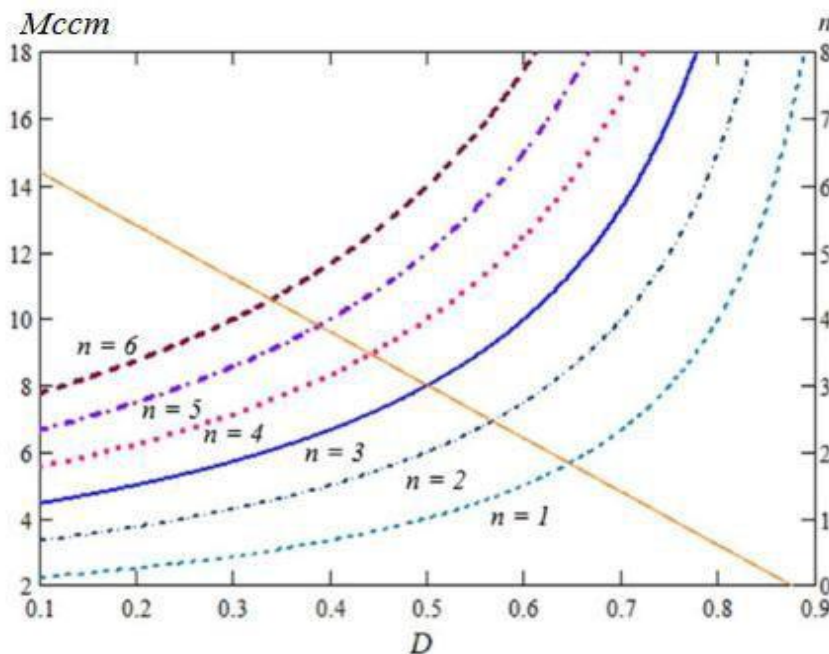


Figure 9: MCCM as a Function of D by Various Turn's Ratios, and the Turn's Ratio Versus Duty Ratio under Voltage Conversion is 8

IV. RESULTS

The proposed Zeta converter with coupled inductor turns proportion of n=3, which is essentially gotten from an ordinary PWM Zeta converter, alongside an inverter is reproduced utilizing simulation programming bundle. The voltage gain is acquired to be 8. For an information voltage of 25V, at 50 KHz the Zeta converter yield voltage is

205V. Along these lines a voltage addition of 8 is accomplished. Air conditioning yield voltage is acquired by associating it to an inverter. The yield waveforms are appeared in Figure. 10 and 11.

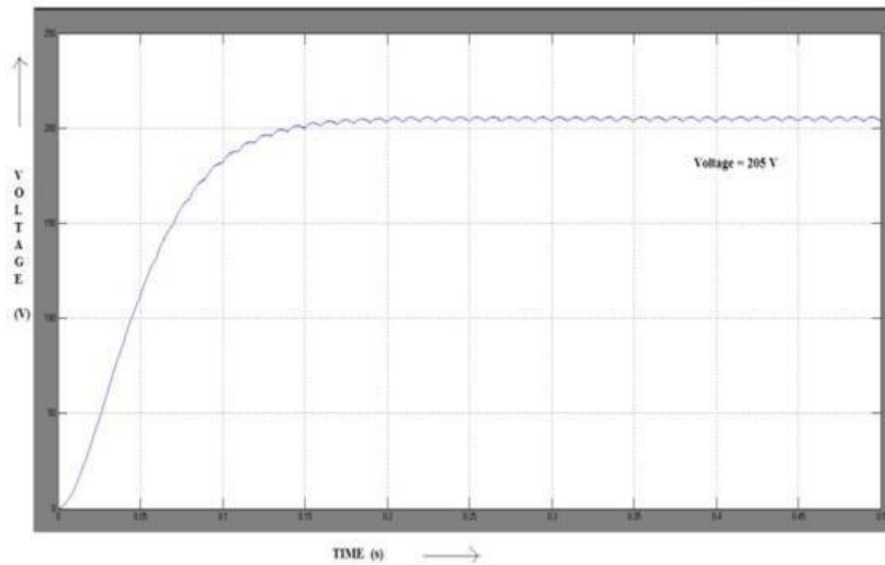


Figure 10: Zeta Converter Output Voltage Waveform

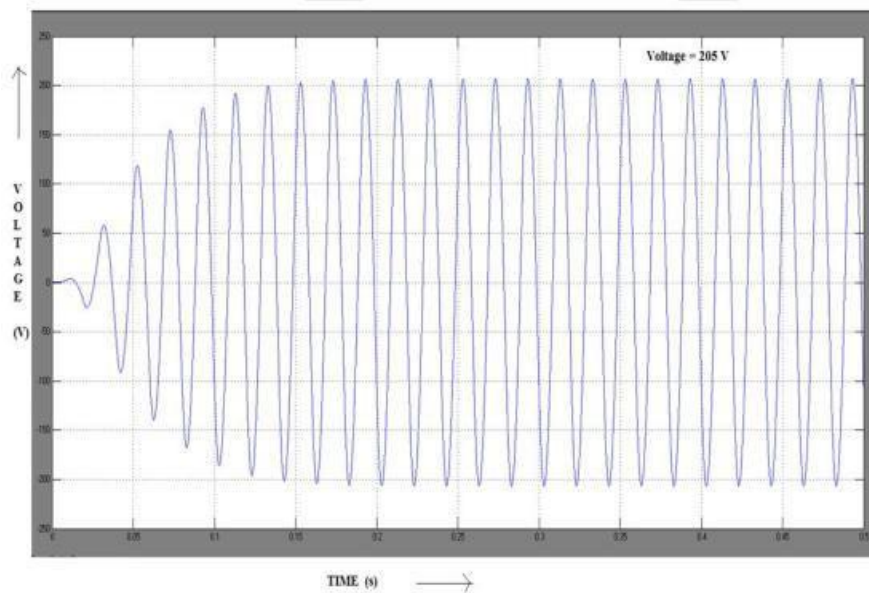


Figure 11: Inverter Output Voltage Waveform

V. CONCLUSION

This paper clarifies a DC/DC Zeta converter with a coupled inductor for the dual-stage micro- inverter. The turns proportion of the coupled inductor expands the voltage gain and the optional twisting of the coupled inductor is in arrangement with an exchanged capacitor for further expanding the voltage. The energy of the leakage inductor of the coupled inductor is reused to the heap by utilizing extra capacitors and diodes. In this way the voltage worry over the dynamic switch is limited and thus low ON-state opposition is gotten. The proposed framework accomplishes a voltage increase of 8 and a productivity of 65% is accomplished.

VI. REFERENCES

- [1] Anun, M., Ordonez, M., Zurbriggen I.G. and Oggier, G.G., "Circular Switching Surface Technique: High-Performance Constant Power Load Stabilization for Electric Vehicle Systems", *IEEE Transactions on Power Electronics*, Vol. 30, No. 8, pp. 4560-4572, 2015.
- [2] Augustine, S., Mishra, M.K. and Lakshminarasamma, N., "Adaptive Droop Control Strategy for Load Sharing and Circulating Current Minimization in Low - Voltage Standalone DC Microgrid", *IEEE Transactions on Sustainable Energy*, Vol. 6, No. 1, pp. 132-141, 2015.
- [3] Barreto, L.H.S.C., Prac, P.P., Oliveira, D.S. and Silva, R.N.A.L., "High - Voltage Gain Boost Converter Based on Three - State Commutation Cell for Battery Charging Using PV Panels in a Single Conversion Stage", *IEEE Transactions on Power Electronics*, Vol. 29, No. 1, pp. 150-158, 2014.
- [4] Bastos, R.F., Aguiar, C.R., Gonçalves, A.F.Q. and Machado, R.Q., "An Intelligent Control System Used to Improve Energy Production From Alternative Sources with DC/DC Integration", *IEEE Transactions on Smart Grid*, Vol. 5, No. 5, pp. 2486-2495, 2014.
- [5] Bautista, S.C., Erbay, C., Han, A. and Sinencio, E.S., "Power Management System with Integrated Maximum Power Extraction Algorithm for Microbial Fuel Cells", *IEEE Transactions on Energy Conversion*, Vol. 30, No. 1, pp. 262-272, 2015.
- [6] Chen, S.M. and Liang, T.J., "A Boost Converter with Capacitor Multiplier and Coupled Inductor for AC Module Applications", *IEEE Transactions on Industrial Electronics*, Vol. 60, No. 4, pp. 1503-1511, 2013.
- [7] Chen, Y.M. and Yu, A.Q.H.X., "A High Step - Up Three-Port DC - DC Converter for Stand-Alone PV/Battery Power Systems", *IEEE Transactions on Power Electronics*, Vol. 28, No. 11, pp. 5049-5062, 2013.
- [8] Choi, B.H., Lee, S.W., Thai V.X. and Rim C.T., "A Novel Single-SiC - Switch - Based ZVZCS Tapped Boost Converter", *IEEE Transactions on Power Electronics*, Vol. 29, No. 10, pp. 5181- 5194, 2014
- [9] Das, P., Pahlevaninezhad, M. and Singh, A.K., "A Novel Load Adaptive ZVS Auxiliary Circuit for PWM Three - Level DC - DC Converters", *IEEE Transa*
- [10] Do, H.L., "A Soft - Switching DC/DC Converter with High Voltage Gain", *IEEE Transactions on Power Electronics*, Vol. 25, No. 5, pp. 1193-1200, 2010.
- [11] Forest, F.O., Meynard, T.A., Labour, E., Gelis B., Huselstein J.J. and Brandelero J.C., "An Isolated Multicell Intercell Transformer Converter for Applications with a High Step - Up Ratio", *IEEE Transactions on Power Electronics*, Vol. 28, No. 3, pp. 1107-1119, 2013.
- [12] Gu, B., Dominic, J., Chen, B., Zhang, L. and Lai, J.S., "Hybrid Transformer ZVS/ZCS DC DC Converter With Optimized Magnetics and Improved Power Devices Utilization for Photovoltaic Module Applications", *IEEE Transactions on Power Electronics*, Vol. 30, No. 4, pp. 2127-2136, 2015.
- [13] Haroun, R., Aroudi, A.E., Pastor, A.C., Garcia, G., Olalla, C. and Salamero, L.M.I., "Impedance Matching in Photovoltaic Systems using Cascaded Boost Converters and Sliding - Mode Control", *IEEE Transactions on Power Electronics*, Vol. 30, No. 6, pp 3185-3199, 2015.
- [14] Hegazy, O., Mierlo, J.V. and Lataire, P., "Analysis, Modeling and Implementation of a Multi device Interleaved DC/DC Converter for Fuel Cell Hybrid Electric Vehicles", *IEEE Transactions on Power Electronics*, Vol. 27, No. 11, pp. 444 - 4458, 2012.
- [15] Hu, K.W., Wang, J.C., Lin, T.S., and Liaw, C.M., "A Switched - Reluctance Generator with Interleaved Interface DC - DC Converter", *IEEE Transactions on Energy Conversion*, Vol. 30, No. 1, pp. 273- 284, 2015.
- [16] Hu, X. and Gong, C., "A High Gain Input - Parallel Output - Series DC/DC Converter with Dual Coupled Inductors", *IEEE Transactions On Power Electronics*, Vol. 30, No. 3, pp. 1306-1317, 2015.
- [17] Khan, M.A., Husain, I. and Sozer, Y., "A Bidirectional DC - DC Converter With Overlapping Input and Output Voltage Ranges and Vehicle to Grid Energy Transfer Capability", *IEEE Journal of Emerging and Selected Topics In Power Electronics*, Vol. 2, No. 3, pp. 507-516, 2014.
- [18] Kong, T.H., Hong, S.W. and Cho, G.H., "A 0.791 mm On - Chip Self - Aligned Comparator Controller for Boost DC-DC Converter using Switching Noise Robust Charge-Pump", *IEEE Journal of Solid - State Circuits*, Vol. 49, No. 2, pp. 502- 512, 2014.
- [19] Lai, C.M., Pan, C.T. and Cheng, M.C., "High - efficiency modular high step - up interleaved boost converter for DC - microgrid applications", *IEEE Transactions on Industry Applications*, vol.48, no.1, pp. 161-171. 2012.